

EUROPEAN ORGANIZATION FOR NUCLEAR RESEARCH

CERN/EP 83-203
23 December 1983

CONFERENCE HIGHLIGHTS AND SUMMATION - EXPERIMENTAL

G. Giacomelli

CERN, Geneva, Switzerland

and

University of Bologna, Bologna, Italy

INFN, Sezione di Bologna, Bologna, Italy

ABSTRACT

The experimental results presented at the "Monopoles 83" Workshop are reviewed and discussed.

Invited paper at the "Monopoles 83" Workshop
Ann Arbor, Michigan, USA, 6-9 October 1983

1. INTRODUCTION

Before 1931 the subject of magnetic monopoles had received little attention in isolated discussions concerning the symmetries of Maxwell's equations, the analysis of the pole-electron system and the magnetic content of matter.

In 1931 Dirac introduced the magnetic monopole in order to explain the quantization of the electric charge [1]. From 1931 till 1974 a number of experimental searches were performed in cosmic rays, at accelerators and in bulk matter in order to find what we may now call the "classical monopole", characterized by a large magnetic charge and a relatively small mass [2]. During the same period, a slightly larger number of theoretical and phenomenological papers tried to resolve some specific problems, like the energy loss of monopoles, the meaning of the "tail" of the monopole, etc.

In 1974 T. Hooft and A.M. Polyakov proved that all gauge theories in which the electromagnetic group $U(1)$ is a subgroup of a larger compact group, predicted the existence of magnetic monopoles with large masses. Since 1974 the number of mathematical and theoretical papers increased considerably; the increase was even greater after 1979, when the main groundworks on Grand Unified Theories (GUT) of electroweak and strong interactions were laid down [3].

The first specific conference on magnetic monopoles, held in Trieste at the end of 1981, was dominated by mathematical developments, though the discussions ranged from physics to mathematics, astrophysics, cosmology and experiments [3].

Experiments searching for GUT (or cosmic) monopoles were somewhat slow to start. But the number of searches increased considerably after the 1982 Stanford candidate event [4].

At the Monopole Workshop held in 1982 at Wingspread, Racine, Wisconsin, USA, many new experimental and theoretical results were presented. An even larger number of papers were presented here in Ann Arbor. It is interesting to note that the experiments have grown in

complexity and that all proton decay experiments are searching for the monopole catalysis of proton decay. The analyses of all types of energy losses of monopoles in matter have become more detailed. There have been many discussions of theories involving gravity and the connections with astrophysics and cosmology have become more numerous.

2. PROPERTIES OF COSMIC MONOPOLES

Let us review briefly the main properties of magnetic monopoles pointing out the recent developments.

2.1 Charge and mass

The magnetic charge g is given by the Dirac relation

$$g = ng_D = \frac{\hbar c}{2e} n = 68.5 e n , \quad (1)$$

where e is the basic electric charge and $n = 1, 2, 3, \dots$. Last year everybody emphasized the values $n = 1$, $e = 1$ and the mass value $m_M \sim 10^{16}$ GeV. At this workshop we were told by theorists that things could be more varied and that one could have several possibilities [5].

$$\begin{aligned} g &= g_D , \quad 10^{16} < m_M < 10^{19} \text{ GeV} , \\ g &= g_D , \quad m_M \sim 10^4 \text{ GeV} , \\ g &= 2g_D , \quad 10^{10} < m_M < 10^{16} \text{ GeV} . \end{aligned} \quad (2)$$

Large masses were emphasized in order to explain the persistence of galactic magnetic fields. Moreover, the Kaluza-Klein theories [6], which could be the basis for bringing also gravity into a unifying picture, may predict $m_M \geq 10^{19}$ GeV and very small radii, so that one could ask if the monopole could be a black hole.

In the following I shall emphasize the results for $m_M \sim 10^{16}$ GeV and $g = g_D$.

2.2 Size and structure

The magnetic pole is pictured as having:

- a core with a radius $r_c \sim 10^{-29}$ cm;
- a region up to $r \sim 10^{-16}$ cm, where virtual W^+ , W^- and Z^0 may be present;
- a confinement region with $r_{con} \sim 1$ fermi;
- a fermion-antifermion condensate region up to $r_f \sim 1/m_f$;
- for r larger than few fermis the monopole behaves as a point Dirac monopole, which generates a magnetic field $B = g/r^2$.

2.3 Flux in cosmic rays

Monopoles should have been produced at the phase transition, which occurred at the cosmic time $t \sim 10^{-35}$ s after the Big Bang, when the unifying gauge symmetry group broke down into smaller subgroups, one of which was $U(1)$. The estimates of the monopole production rates in the simplest GUT models are too large; estimates based on modified GUT models, in particular in "inflationary" models, may lead to very small rates. One may conclude that present production models are of little guidance, since the estimated production rates may range from zero to very large values [5].

The constraint in the monopole flux obtained from the condition that the monopole mass density be smaller than the critical mass density, that is the density which would close the universe, is $F < 5 \times 10^{-5}$ poles $\text{cm}^{-2} \text{s}^{-1} \text{sr}^{-1}$ if one assumes $m_M \sim 10^{16}$ GeV and that the monopole density in the universe is uniform. The upper limit becomes 10^5 times larger if the monopoles are assumed to be clumped in galaxies like the other types of matter.

The bounds obtained from the existence of magnetic fields in most celestial bodies, in particular in our galaxy, lead to stronger constraints on the monopole flux: from the galactic field one has: $F < 10^{-15} \text{ cm}^{-2} \text{s}^{-1} \text{sr}^{-1}$ if $m_M < 10^{17}$ GeV (Parker bound). The limit which may be obtained from the existence of a magnetic field in the local supercluster is more doubtful, but could be an order of magnitude smaller.

We have heard that magnetic fields are present in essentially all celestial bodies and that from all of them one can obtain limits on monopole fluxes. It seems that these magnetic fields originate from a continuous dynamo mechanism, determined by the large scale fluid motion; for instance, for our galaxy the magnetic galactic field is stretched in the azimuthal direction along the spiral arms and it is due to the non-uniform rotation of the galaxy. This generates the field with a time scale approximately equal to the rotation period of the galaxy ($\tau \sim 10^8$ years). Though this mechanism seems plausible, there still are uncertainties and the picture is not completely settled. For instance, a primordial magnetic field could give some effect.

One could ask where could the monopoles be. One could ask if they could contribute to the dark matter, in particular to that which surrounds the galaxies and forms their halos. It has to be kept well in mind that $\sim 90\%$ of the matter in the universe is not visible. One could also ask if the monopoles cluster like ordinary matter on planetary systems, thus yielding local enhancements. It seems that this is possible, but that the enhancement over the galactic flux could at most be an order of magnitude (and probably only a factor of 2-3). I recall that last year one thought that the enhancement could be much larger.

On the basis of what has been said above one can expect that on earth could arrive a flux of cosmic poles as sketched in fig. 1. Note that one could have high velocity poles ($\beta > 3 \times 10^{-3}$, extragalactic flux), poles with $\beta \sim 3 \times 10^{-3}$ bound in the local supercluster, poles with $\beta \sim 10^{-3}$ bound in the galaxy, poles with $\beta \sim 10^{-4}$ bound in the solar system, etc. The flux should increase with decreasing pole velocity, down to $\beta \sim 3 \times 10^{-5}$, which is the escape velocity of the earth. Clearly, the graph is only indicative. Compared to the ideas of one year ago [4] it would seem that the local flux of low velocity monopoles has decreased, while the flux of high energy poles has increased. We have also heard of poles which could enter in some magnetic flux tubes in neutron stars and be accelerated up to $\beta \sim 0.1$ [7].

2.4 Monopolonium

Some monopoles may be trapped into a pole-antipole system, which because of the large pole mass, would have a very long lifetime. Not much new has been added to this subject. It has been restated that one could have of the order of 10^3 pole-antipole annihilations per year on a volume of $(1 \text{ light year})^3$. These annihilations would lead to fantastic events, with thousands or millions of secondary particles, where would be present all the known and all the unknown particles of high energy physics [8].

2.5 Capture of an atomic nucleus

The long range electromagnetic interaction of a magnetic charge with the dipole magnetic moment of a nucleus may yield a pole-nucleus bound system (plus the emission of energy). G. Fiorentini [9] has estimated that these "monopolic atoms" have binding energies in the range 1-100 KeV, with typical linear sizes of the order of 20 fermi. C. Goebel [10] has estimated that the capture cross section of the Al^{27} nucleus by a monopole with $\beta \sim 10^{-3}$ could be $\sim 0.3 \text{ mb}$. This corresponds to a mean free path in earth of $\sim 5 \text{ km}$, considering an average abundance of Al in the earth crust. A sizable number of poles moving in the galaxy should have attached a proton. When traversing a few kilometers of earth a sizable number of poles, which do not already have an attached nucleus, should attach aluminium nuclei.

The formation of "monopolic atoms" could affect the effective cross section of the catalysis of proton decay by monopoles.

3. DETECTION OF COSMIC MONOPOLES

We shall now discuss the results of the searches performed with various methods of detection: induction techniques, scintillation counters, proportional chambers, plastic detectors and indirect methods. The knowledge of the energy loss of slow monopoles is crucial for most methods of detection; it is also controversial for poles with $\beta < 10^{-3}$. [11-13].

3.1 Superconducting induction devices

A monopole passing through a superconducting coil induces a change of magnetic flux connected with the coil and thus a change in the electric current in the superconducting coil. This method of detection is ideal since it is based solely on the long range electromagnetic interaction between the moving magnetic charge and the macroscopic quantum state of the superconducting ring. The method is independent of the monopole mass, velocity and electric charge.

After the pioneering work of the Berkeley group [14], the Stanford Group operated successfully in 1982 a single coil of 20 cm^2 area [15]. Now several experimental groups have in operation what may be called second generation experiments, characterized by areas one order of magnitude larger, coincidence arrangements and sophisticated procedures for eliminating spurious events [16]. Examples of these detectors are the 3-axis detector at Stanford (fig. 2), the seventh order gradiometer at IBM (fig. 3), and the "macrame" arrangement at Chicago (fig. 4). It may be worth recalling that the fraction of signal collected is limited not by detector size, but by the size of each loop. Fig. 5 shows the chart recording of the currents in the three loops of the Stanford detector. It also shows the recording of an accelerometer, which should help in eliminating possible "candidates", in reality caused by mechanical disturbances.

Experimental results have been presented at this workshop by several groups, as listed in table 1. After the candidate event reported in 1982 by the Stanford group, no other candidate was observed. The present level is $\sim 1/60$ th of that reported by Stanford in 1982.

3.2 Energy losses of monopoles

At high velocities, $\beta > 10^{-2}$, the interaction of poles with matter is well understood: a pole of magnetic charge g behaves as an equivalent electric charge $e_{\text{eq}} = g\beta$. The energy loss, due to impact ionization, is described by the Bethe-Bloch formula. For liquid hydrogen the result is the curve c of fig. 6 [13, 17-18].

For smaller velocities, $10^{-4} < \beta < 10^{-3}$, the energy losses are mainly due to adiabatic excitation of the atoms, arising from the interaction of the atomic electrons with the monopole magnetic field. In this case crossing of the atomic levels may occur (fig. 7). The net effect is that the passage of a monopole may leave atoms in an excited state. This is the "Drell" effect, which until now has been computed only for atomic hydrogen and helium [17]. The curve b in fig. 6 shows the energy loss due to the Drell effect in hydrogen. The effect may be used for practical detection either by observing the photons emitted in the de-excitation of the excited atom or by observing the ionization caused by the energy transfer from the excited atoms to complex molecules with a small ionization potential (Penning effect). If the monopoles has attached a charged particle (or if it is a dyon) the Drell effect could be reduced.

The Drell mechanism is effective as long as the monopole-atom collision energy exceeds the spacing of atomic levels. For smaller energies, that is for smaller β , the energy loss is due to elastic monopole-atom collisions arising from the long range magnetic charge-magnetic dipole interaction. The energy is eventually dissipated into heat. Curve a of fig. 6 shows the energy loss due to elastic collisions in liquid hydrogen [13].

For materials more complex than liquid hydrogen one expects energy losses which are qualitatively the same, but which should interest lower velocities. Thus the curves b and c of fig. 6 should shift toward lower β , by even an order of magnitude in β [11-12].

Ahlen et al [11, 19-20] have pointed out that when using scintillators one cannot limit the considerations to the ionization energy loss, but one should consider the photon yield and the saturation effect in solids. They have obtained the photon yield shown in fig. 8 for a pole, a dyon and a pole + Al nucleus traversing a plastic scintillator. The curves show that there is an effective threshold at $\beta \sim 5 \times 10^{-4}$. The calculations of other authors [12] would indicate a sensitivity down to $\beta \sim 10^{-4}$. The curves of fig. 8 represent in any case a lower bound on the light yield, since there must be other effects, like those discussed above due to the magnetic charge-magnetic dipole interaction, which may effectively shift the β -threshold.

3.3 Detection with scintillation counters and proportional chambers

Table 2 gives a comprehensive summary of the electronics experiments and of the upper limits achieved for the β -range covered [4,20].

Besides the early experiments performed with two or more layers of scintillation counters and/or proportional chambers, in the last year a number of new methods were developed and applied to cosmic monopole searches. These methods will now be briefly discussed (table 2 gives the relevant parameters also for these experiments).

The Tokyo Group [21] used a stack of scintillation counters and of proportional chambers, employing 90% gaseous helium and 10% CH_4 , fig. 9. In the proportional chambers the monopoles could excite the helium atoms via the Drell mechanism discussed in sect. 3.2



Then, by the Penning effect, the excitation energy of the excited He^* is transferred into ionization of the CH_4 molecule



Therefore, one may obtain an effective ionization also for low velocity monopoles, in the $10^{-4} < \beta < 10^{-3}$ range.

The Berkeley-Indiana Group [19] used a single thick slab (7.6 cm) of scintillator. Relativistic charged particles traverse the detector in a time much shorter than the response time of the detector system (~ 40 ns). A GUT pole travelling with $\beta = 10^{-3}$ takes at least 250 ns to traverse the scintillator. The signature of a monopole is thus given by an anomalously wide pulse with a constant pulse height in time. With this arrangement the experimenters should have reached the β limit given by ionization energy losses.

The Mont-Blanc detector for proton decay [22] is a cubic detector of 3.5 m side, made of 134 layers of limited streamer tubes, separated by 1 cm thick iron absorbers. The detector is capable of determining the path of an eventual monopole with a transverse precision of $\sim 1 \text{ cm}^2$.

The identification may be made by time-of-flight through the whole detector. The authors point out that because of the many samplings involved the apparatus is capable of detecting monopoles which ionize $1/100$ of I_{\min} because of the Landau tail in the energy loss distribution.

Fig. 10 shows a compilation of upper limits (at the 90% confidence level) for a flux of cosmic GUT poles plotted versus the β of the monopole.

3.4 Detection with track-etch detectors

Track-etch detectors may be considered as threshold devices with thresholds which depend on the material and on the method of chemical etching. Approximate thresholds for monopoles are: CR 39: $\beta > 0.02$; nitrocellulose: $\beta > 0.04$; lexan (makrofol E): $\beta > 0.3$; mica: $\beta > 2$. These detectors may be exposed for long times (longer than one year). The passage of a heavily ionizing particle produces a number of defects along its path. Since the plastics are good insulators these defects last for long times. The plastics are then chemically etched: the passage of a charged particle may appear as a hole in the plastic if it was heavily etched, or as a cone on each side of the plastic if the etching was moderate.

A Berkeley Group [23] exposed $\sim 15 \text{ m}^2$ of several layers of CR39 for about one year at ground level. They quoted an upper limit $F < 1.5 \times 10^{-13} \text{ cm}^{-2} \text{ s}^{-1} \text{ sr}^{-1}$ for $\beta > 0.02$.

A Japanese Group [24] exposed 100 m^2 of nitrocellulose sheets for 3.3 years at ground level at Kitami, Hokkaido. The experiment was originally designed to search for "classical monopoles". It was modular, with each unit consisting of a stack of a pair of nitrocellulose sheets, a pair of polycarbonate sheets and an x-ray film. Only the nitrocellulose is useful for the detection of relatively slow poles. The authors quoted an upper limit $F < 5.2 \times 10^{-15} \text{ cm}^{-2} \text{ s}^{-1} \text{ sr}^{-1}$ for poles with $\beta > 0.04$.

3.5 Catalysis of proton decay

It was suggested in 1980 that a GUT monopole in proximity of hadronic matter could catalyze baryon number violating processes such as

$$p + M \rightarrow M + e^+ + \text{mesons} . \quad (5)$$

It was thought that the cross section would be very small, comparable to the geometrical cross section of the core ($\sim 10^{-58} \text{ cm}^2$), where may be found the X-mesons which mediate the $\Delta B \neq 0$ interactions. In 1982, V.A. Rubakov [25-26] and C.G. Callan [27] suggested that the cross section could be comparable to the cross section of ordinary strong interactions ($\sigma \sim 10^{-26} \text{ cm}^2$) because the monopole should be surrounded by a condensate of fermion-antifermion pairs. This possibility has stirred up considerable theoretical interest and many controversies. At this time one should in fact consider the cross section to be uncertain by several orders of magnitude.

If the $\Delta B \neq 0$ cross section for monopole catalysis of the proton decay would be large, then a monopole would trigger a chain of baryon "decays" along its passage through a large detector, such as those designed to study baryon decay. The mean free path λ between two successive monopole-induced proton decays would be for slow monopoles

$$\lambda \text{ (m)} = \frac{43}{\rho \text{ (g cm}^{-3}\text{)} \sigma} \beta , \quad (6)$$

where σ is the cross section in units of the typical strong interaction cross section ($\sigma_0 = 4 \cdot 10^{-26} \text{ cm}^2$), β the velocity of the pole and ρ the density (in g cm^{-3}) of the material traversed. Note that in (6) one has assumed that $\sigma_{\text{cat}} \sim 1/\beta$.

While one year ago there were only some rough upper limits from the analysis of bubble chamber pictures and indirect information, now most of the large scale proton decay experiments have reported upper limits for the monopole catalysis of proton decay. Table 3 lists some of the main features of these experiments together with the measured upper limits [28]. Some limits are shown in more detail in figs 11 and 12.

The Aachen-Hawaii-Tokyo Group performed a quick experiment using a water Cherenkov counter filled with 12 t of water. From a 12 day run they obtained an upper limit flux of $2 \times 10^{-12} \text{ cm}^{-2} \text{ s}^{-1} \text{ sr}^{-1}$ valid for $5 \times 10^{-4} < \beta < 5 \times 10^{-2}$ [28].

The Mont-Blanc proton decay detector, which was already mentioned in the previous section, has an average density of 3 g cm^{-3} . It is located under Mont-Blanc at a depth of 5000 m of water equivalent [22].

The Irvine-Michigan-Brookhaven (IMB) water Cherenkov detector is a parallelepiped of $17 \times 22.5 \times 18 \text{ m}^3$, viewed by 2048 photomultipliers. It is located at a depth of 600 m ($\sim 2000 \text{ m}$ of water equivalent) in the Morton salt mine near Cleveland, Ohio [29].

The Soudan-1 prototype consists of horizontal layers of 3456 proportional tubes each 4 cm in deameter, held in a matrix of taconite (iron loaded concrete). The average density of the detector is 1.6 g cm^{-3} ; the detector is $2.9 \times 2.9 \times 1.9 \text{ m}^3$ and wheighs 31 t [28].

The Tokyo water Cherenkov counter is a cylinder of 15 m diameter and 16 m height. They use very large photomultipliers which were specifically designed for the experiment [28].

The Tata-Osaka-Tokyo detector is composed of 34 layers of proportional counters with 1.2 cm iron plates between the layers. The counters are $10 \times 10 \text{ cm}^2$ area by 4 or 6 m length. The detector is a $6 \times 4 \times 3.7 \text{ m}^3$ parallelepiped with a total wheight of 140 t and an average density of 1.6 g cm^{-3} [28].

Stringent indirect limits on catalysis were obtained by various authors considering the catalysis of nuclear matter within neutron stars. The upper limits were obtained by looking at the general x-ray background and at the x-ray emission for some particular neutron star. The limits (on monopole flux times catalysis cross section times the β of the monopole) are of the order $F \propto \beta < 10^{-50} \text{ s}^{-1} \text{ sr}^{-1}$ [7, 30]. This value could possibly be modified by unknown properties and structure of the neutron stars.

3.6 Other methods of detection

(a) Searches in bulk matter

As already stated in sect. 2, magnetic monopoles could be trapped in ferromagnetic domains by an image force of the order of 10 eV/\AA . Cosmic poles of low velocity ($\beta < 10^{-4}$) could have stopped in ferromagnetic materials at the surface of the earth, after traversing it. The probability for stopping is very small. On the other hand some ferromagnetic deposits were formed hundreds of millions of years ago, so that accumulation over long times may have occurred.

The Kobe Group has performed a search for relic monopoles trapped in iron sand using several tens of kilograms of material formed between 10^7 and 10^8 years ago [31]. The sand was heated above the Curie point at which temperature the material stops being ferromagnetic. The poles, which were trapped in the material, would leave it, would fall towards the earth and would be detected in a superconducting induction coil through which they would pass. The Kobe Group placed the upper limit of 2×10^{-6} poles per g of ore. It is difficult to extract from this an upper limit on the monopole flux: it is estimated to be of the order of 10^{-13} poles $\text{cm}^{-2} \text{ s}^{-1} \text{ sr}^{-1}$ for poles with $\beta < 10^{-4}$.

A Wisconsin Group is proposing to perform an experiment of this type on a large scale, using the ancient iron ore processed in a steel mill in Wisconsin.

(b) Searches for ancient tracks in mica

Mica as a track-etch detector has a high threshold (it would not detect even relativistic monopoles with $n = 1$). On the other hand, it should detect the passage of a "monopolic atom", when the attached nucleus is for instance aluminium, if the speed of the system is of the order of $10^{-3} c$, where ionization losses of charged particles are largest.

Ahlen et al. [20] have taken a piece of mica from a mine 5 km deep in Brazil. The age of the mica was estimated to be $\sim 4.6 \times 10^8$ years. The authors emphasize that the damage in the mica is caused by nuclear stopping power. After etching in hydrofluoric acid they scanned

with an optical microscope 14 cm^2 of mica. They estimated an upper limit $F < 2 \times 10^{-17} \text{ cm}^{-2} \text{ s}^{-1} \text{ sr}^{-1}$ for poles with $4 \times 10^{-4} < \beta < 2 \times 10^{-3}$. These limits are obtained assuming that the poles may attach an Al nucleus and that the mean free path for Al attachment in the earth crust be $\sim 5 \text{ km}$. It is not clear what would happen if the monopoles would have attached already a light nucleus, like a proton.

(c) Other detectors

With a detailed calculation De Rujula has shown that a monopole traversing a metal produces a "thermo-acoustic" pulse, whose amplitude is linear in the monopole's velocity [32] (fig. 13). If the metal is superconducting, there is a novel additional "magneto-acoustic" source whose amplitude is β -independent. He sketched a "sonic antenna" that could respond directionally to monopoles (and even to normal particles of cosmic rays, and to more exotic objects), (fig. 14).

More conventional acoustic detectors applied to metal slabs at room temperature were discussed by Barish [33].

Though not yet operational, acoustic and thermo-acoustic detectors show promise for the future detection of low β monopoles.

Induction coils at room temperature have been discussed by Price [34]. Also these detectors are about to become operational.

4. EXPERIMENTS AT ACCELERATORS

At present the main emphasis of monopole searches concerns cosmic GUT monopoles. Nevertheless, given the global uncertainty in the field, searches are still made at the highest energy accelerators for what may be called "classical" monopoles. In practice one hypothesizes that monopoles have relatively low masses so that they can be produced in reactions of the type

$$\begin{aligned} p + p &\rightarrow p + p + g + \bar{g} , \\ \bar{p} + p &\rightarrow g + \bar{g} , \\ e^+ + e^- &\rightarrow g + \bar{g} , \end{aligned} \tag{7}$$

where \bar{g} is an antimonopole.

Recent searches have been performed at the e^+e^- storage rings PEP [35] and PETRA [36] and the $\bar{p}p$ Collider at CERN [37]. In these experiments the CR39 plastic detectors were used. Sheets of this material surrounded an intersection region. Heavily ionizing relativistic monopoles should have crossed some of the plastic sheets, where they should have left defects. When properly developed, the sheets should show holes along monopole tracks. The experiments at the e^+e^- storage rings placed an upper limit cross section of $\sim 10^{-37} \text{ cm}^2$, which is about three orders of magnitudes smaller than the QED cross section for point particles. Thus these experiments would exclude poles with masses up to about 16 GeV. The experiment at the CERN $\bar{p}p$ Collider, using kapton foils inside the vacuum chambers and CR39 outside, established an upper limit of $\sigma < 3 \times 10^{-32} \text{ cm}^2$ for monopole masses up to 150 GeV.

Fig. 15 summarizes as a function of the monopole mass the production cross section upper limits (at the 95% confidence level). Solid lines refer to "direct" measurements (such as those discussed above); dashed lines refer to "indirect" measurements (where monopoles should have been stopped and trapped in ferromagnetic materials; later they would have been extracted and accelerated by strong magnetic fields and detected).

5. CONCLUSIONS AND OUTLOOK

At this workshop we have learned that the list of what monopoles can do has become longer. They may catalyze proton decay, induce nuclear fission of heavy elements, induce β decay, attach nuclei, destroy magnetic fields, etc.; one should probably also mention the possible "induction of lightning" and the "problem of perpetual motion" according to Peter Peregrinus, in 1269!. We have also learned that the monopole could be so massive that it could be a minuscule black hole. Moreover, monopoles could be part of the dark matter in the universe; alternatively they could be so few as to be undetectable.

It is clear that the field of magnetic monopoles has evolved into a fascinating interdisciplinary field of physics, with implications in fundamental theories, in particle physics, in astrophysics and cosmology. In certain aspects it represents a connection between physics and cosmology.

The theoretical and phenomenological understanding of monopoles has improved considerably in the last few years. But new possibilities have opened up. I refer in particular to the various differing predictions of the monopole mass and of the monopole production rates in the early universe. Therefore, theoretical guidance to experiments is not really adequate.

From the experimental point of view, one clearly observes the trend towards larger and costlier experiments. Moreover, it has been pointed out by several people, in particular by Frisch, that in the searches for rare events it is normal to get a candidate, which is difficult to reject. This forces the experimenters to use at the same time, at least in large layouts, more than one technique in order to obtain redundancy and gain in "convincingness" [16, 38].

The present trend towards larger experiments may be summarized as follows:

Induction experiments: some groups are planning layouts with 1-10 m² coils.

Electronics experiments: the present largest experiments are the following: Baksan ($S\Omega = 1800 \text{ m}^2\text{sr}$), Mont-Blanc liquid scintillator detector ($700 \text{ m}^2\text{sr}$), Homestake ($1300 \text{ m}^2\text{sr}$), Texas A & M ($300 \text{ m}^2\text{sr}$), Fréjus ($1000 \text{ m}^2\text{sr}$). There are plans for layouts with $\sim 1000 \text{ m}^2$ active detectors at Stanford, Michigan and Italy (Gran Sasso) [39-40].

Plastic detectors: in the Kamioka mine the Japanese are installing 1000 m^2 of CR39 [40].

Catalysis of proton decay: all proton decay experiments have installed new electronics and are improving it in order to be able to detect a string of catalyzed proton decays.

But what if one finds nothing? To overcome this question several of the larger experiments are planning to add "worthy byproducts", like detection of multimMuon events (muon bundles), neutrinos from supernovae explosions, etc. But what the field of monopole really requires would be some real monopoles!

Acknowledgements

I would like to acknowledge many colleagues for discussions and for sending material before publication. In particular, I would like to thank Drs. B. Cabrera, P. Capiluppi, R.A. Carrigan Jr, D. Cline, A. De Rujula, G. Fiorentini, M. Koshiha, G. Mandrioli, P. Musset, A.M. Rossi and J. Stone.

REFERENCES

- [1] P.A.M. Dirac, Quantized singularities in the electromagnetic field, Proc. Roy. Soc. 133 (1931) 60.
- [2] G. Giacomelli, Searches for missing particles, Invited paper at the 1978 Singapore Meeting on "Frontiers of Physics", Proceedings of the Conference (1978).
- [3] G. Giacomelli, Review of the experimental status (past and future) of monopole searches, Proceedings of the Conference on "Monopoles in quantum field theory", Trieste (1981).
- [4] G. Giacomelli, Experimental status of monopoles, Proceedings of the 1982 Wingspread Workshop (1982).
- [5] E.J. Weinberg, Monopoles and Grand Unification, this Workshop.
- [6] M.L. Perry, Monopoles in Kaluza-Klein theories, this Workshop.
- [7] E.W. Kolb, Experimental limits on monopole catalysis, this Workshop.
- [8] C.T. Hill, Monopolonium, Nucl. Phys. B229 (1983) 469.
- [9] G. Fiorentini, Binding of magnetic monopoles and atomic nuclei, this Workshop.
- [10] C. Goebel, Vacuum anti-shielding of magnetic charge, this Workshop; Binding of monopoles to nuclei, this Workshop.
- [11] S.P. Ahlen and G. Tarlé, Can grand unification monopoles be detected with plastic scintillators?, Phys. Rev. D27 (1983) 688.
- [12] D.M. Ritson, Magnetic monopole energy losses, SLAC-PUB-2950 (1982).
- [13] L. Bracci et al., On the energy loss of very slowly moving magnetic monopoles, IFUP-TH 83/26 (1983).
- [14] L.W. Alvarez et al., A magnetic monopole detector utilizing superconducting elements, Rev. Sci. Instr. 4 (1971) 326.
- [15] B. Cabrera, First results from a superconducting detector for moving magnetic monopoles, Phys. Rev. Lett. 48 (1982) 1378.
- [16] H. Frisch, Monopole detection by induction techniques, this Workshop.
- [17] S.D. Drell et al., Energy loss of slowly moving magnetic monopoles in matter, Phys. Rev. Lett. 50 (1983) 644.
- [18] S. Geer and W.G. Scott, Calculation of the energy loss for slow monopoles in atomic hydrogen, CERN pp Note (1981).
- [19] G. Tarlé et al., First results from a sea level search for supermassive magnetic monopoles, report presented at this Workshop.

REFERENCES (Cont'd)

- [20] S. Ahlen, Monopole detection by ionization/excitation techniques, this Workshop.
- [21] F. Kajino et al., A scintillator-proportional counter search for monopoles, this Workshop.
- [22] G. Battistoni et al., Nucleon stability, magnetic monopoles and atmospheric neutrinos in the Mont-Blanc experiment, CERN/EP 83-147 (1983).
- [23] P.B. Buford-Price, Searches for exotic particles, Proceedings of the Wingspread workshop on magnetic monopoles (1982).
- [24] T. Doke et al., Search for massive magnetic monopoles by plastic track detectors, Phys. Lett. 129 B (1983) 370.
- [25] V.A. Rubakov, Superheavy magnetic monopoles and decay of the proton, JETP Lett. 33 (1981) 644.
- [26] V.A. Rubakov, Adler-Bell-Jackiv anomaly and fermion number breaking in the presence of a magnetic monopole, Nucl. Phys. B203 (1982) 311.
- [27] C.G. Callan Jr., Dyon-fermion dynamics, Phys. Rev. D26 (1982) 2058; Monopole catalysis cross sections, this Workshop.
- [28] S. Errede, Experimental limits on monopole catalysis, this Workshop.
- [29] S. Errede et al., Experimental limits on magnetic monopole catalysis of nucleon decay, Phys. Rev. Lett. 51 (1983) 245.
- [30] K. Freese, Monopoles in pulsar 1929.10, this Workshop.
- [31] T. Ebisu and T. Watanabe, Search for superheavy monopoles in 65 kg of iron magnetic sand with a SQUID fluxmeter, Journal Phys. for Japan 52 (1983) 2617.
- [32] C. Bernard, A. De Rujula and B. Lautrup, Sonic search for monopoles, gravitational waves and newtorites, CERN/TH 3694 (1983).
- [33] B. Barish, The physics of monopole detection, this Workshop.
- [34] M.J. Price, The detection of cosmic monopoles using a room temperature coil, CERN/EP 83-2 (1983).
- [35] K. Kinoshita et al., Search for highly ionizing particles in e^+e^- collisions at $\sqrt{s} = 29$ GeV, Phys. Rev. Lett. 48 (1982) 77.
- [36] P. Musset et al., Search for magnetic monopoles in e^+e^- collisions at 34 GeV c.m. energy, Phys. Lett. B128 (1983) 333.
- [37] B. Aubert et al., Search for magnetic monopoles in $\bar{p}p$ interactions at 540 GeV c.m. energy, Phys. Lett. 120B (1983) 465.

REFERENCES (Cont'd)

- [38] G. Charpak, Detectors for rare events, this Workshop
- [39] D. Ritson et al., Helium proportional chamber monopole detector, this Workshop.
- [40] J. Van der Velde, AMMANDA, an advanced monopole, muon and neutrino detector array, this Workshop.
- [41] K. Kavagoe et al., A search for magnetic monopoles with 1000 m² of plastic track detector, Status report, this Workshop.

TABLE CAPTIONS

Table 1 List of experiments searching for cosmic monopoles using superconducting induction devices [13]. The table gives for each group the main feature of the apparatus, the effective area for which one has a 4π solid angle and the flux upper limit (90% confidence level; the first value corresponds to one event). The overall combined upper limit is $1.5 \times 10^{-11} \text{ cm}^{-2} \text{ s}^{-1} \text{ sr}^{-1}$.

Table 2 List of experiments which searched or are searching for a flux of cosmic monopoles with scintillation counters, proportional tubes and track-etch detectors [19-24].

Table 3 Some of the main features of the large proton decay experiments and upper limits on the monopole flux. These are at the 90% confidence level and were obtained assuming $\sigma_{\text{cat}} = 10 \text{ mb}$. The upper limits from the no observation of a string of interactions (≥ 2) are the most significant; for these the table quotes also the β range covered. The upper limits from single interactions are limited by the general background from neutrino interactions.

TABLE 1

Group	Main feature	Area ($\text{cm}^2/4\pi$)	Flux limit ($10^{-11} \text{ cm}^{-2} \text{ s}^{-1} \text{ sr}^{-1}$)
Stanford 1	Single coil	10	61
Stanford 2	3 axis coils	71	2
Chicago FNAL-Mich.	2 coils	700	7
IBM - 1	Gradiometer	25	51
IBM - 2	Gradiometer	1000	-
Kobe	2 coils	25	200
IC	2 coils	300	-
NBS	Backgr. studies	-	-

TABLE 2

Laboratory	Location	Detector	ΩS (m^2 sr)	dE/dx (minimum)	β range	Flux upper limit ($cm^{-2} s^{-1} sr^{-1}$)
1. BNL	Building	Proportional	1.9	2.0	$3 \times 10^{-4} - 1.2 \times 10^{-3}$	3.4×10^{-11}
2. Bologna	Building	Scintillators	10-36	10-25	$10^{-3} - 0.6$	3.4×10^{-13}
3. Tokyo	Building	Scintillators	1.1	1.2	$10^{-2} - 10^{-1}$	1.5×10^{-11}
"	Building	Scintillators	1.4	0.025	$2 \times 10^{-4} - 5 \times 10^{-3}$	1.5×10^{-11}
"	Kamioka mine	Scintillators	22.0	0.2	$6 \times 10^{-4} - 1$	1.5×10^{-12}
4. Michigan	Building	Scintillators	11.0	0.01-0.05	$3 \times 10^{-4} - 10^{-2}$	8.1×10^{-11}
5. Utah-Stanford	Mayflower mine	Scintillators	2.7	0.12	$1.4 \times 10^{-4} - 3 \times 10^{-2}$	8.1×10^{-12}
6. Minnesota-Argonne	Soudan mine	Proportional	71.6	0.5	$4 \times 10^{-4} - 3 \times 10^{-2}$	4.1×10^{-13}
7. USSR	Baksan mine	Scintillators	1800.0	0.25	$4 \times 10^{-3} - 5 \times 10^{-2}$	1.5×10^{-14}
8. India - Japan	Kolar mine	Proportional	218.0	2.5	$2 \times 10^{-3} - 0.9$	3.5×10^{-14}
9. Mont-Blanc	Tunnel	Streamer tubes	12.0	0.02	$3 \times 10^{-4} - 0.5$	1.9×10^{-12}
10. BNL-Brown-KeK	Neutrino beam	Drift + Scint.	14.5	0.3	$10^{-3} - 0.2$	5.2×10^{-12}
11. Tokyo	Building	Scint + Drell	24.7	-	$> 2 \times 10^{-4}$	1.6×10^{-12}
12. Berkeley-Indiana	Building	Scintillator	17.5	1.2	$6 \times 10^{-4} - 2.1 \times 10^{-3}$	4.1×10^{-13}
13. Berkeley	Surface	CR39	150.0	Z/ $\beta \geq 30$	0.02 - 1	1.5×10^{-13}
14. Kitami	Building	Nitrocellulose	1000.0	Z/ $\beta \geq 60$	0.04 - 1	5.2×10^{-15}

TABLE 3

Collaboration	Location	Depth (m of H ₂ O)	Dimension (m ³)	Effective surface (m ²)	Effective height (m)	Run time (years)	Upper limits for $\sigma = 10\text{mb}$ ($\text{cm}^{-2} \text{ s}^{-1} \text{ sr}^{-1}$) ≥ 2 interactions	Approximate β - Range for ≥ 2 interactions
Tata-Osaka Tokyo	Kolar gold mine	7600	6 x 4 x 3.7	30	2.5	2.4	3×10^{-12}	$10^{-3} - 10^{-1}$
Frascati-Milan Torino	Mont-Blanc tunnel	5000	(3.5) ³	18	2.3	1.2	2.3×10^{-14}	$10^{-3} - 4 \times 10^{-2}$
Irvine-Michigan Brookhaven	Morton salt mine	1500	17 x 22.5 x 18	550	12.8	0.6	3.6×10^{-15}	$6 \times 10^{-4} - 10^{-1}$
Tokyo-LICEPP	Kamioka mine	2700	15 \emptyset x 16	218	10.3	0.2	3.8×10^{-14}	$10^{-4} - 4 \times 10^{-3}$
ANL-Minesota	Soudan mine	1800	2.9 x 2.9 x 1.9	10	1.7	0.8	1.5×10^{-13}	$> 10^{-3}$

FIGURES CAPTIONS

- Fig. 1 Sketch of the possibly expected flux of cosmic monopoles versus their β . The various peaks correspond to poles trapped locally (to the sun and the earth), to poles trapped in the galaxy and to extragalactic poles.
- Fig. 2 Schematic top view of the Stanford three-loop superconducting monopole detector [13].
- Fig. 3 Schematic top view of IBM 7th order superconducting gradiometer [13].
- Fig. 4 "Macrame" superconducting structure of the Chicago coil [13].
- Fig. 5 Chart recording of the loops and of the accelerometer of Stanford-2 detector [13]. Note the disturbances generated at the time of the liquid nitrogen transfer in the outer cryostat.
- Fig. 6 The energy loss (in MeV/cm) of monopoles in liquid hydrogen as function of β [16-18]. Curve (a) corresponds to elastic monopole-hydrogen atom scattering [16]; curve (b) corresponds to adiabatic interaction with level crossings [17] and Curve (c) describes the ionization loss [18]. The dashed parts of the curves correspond to velocity ranges where the approximations used in the calculations may break down.

FIGURES CAPTIONS (Cont'd)

- Fig. 7 The energy levels for atomic hydrogen before (left), during (centre) and after (right) the passage of a magnetic monopole [17].
- Fig. 8 Scintillation light yield for monopoles in an acrylic scintillator as a function of β [14-19].
- Fig. 9 Layout of the new Tokyo detector, which uses the Drell and Penning effects (see text) [21].
- Fig. 10 Compilation of upper limits for a flux of cosmic GUT monopoles plotted versus the β of the monopoles. The Stanford-1 Experiment corresponds to one candidate event; the other experiments are upper limits at the 90% confidence level. Most limits were obtained with scintillation or gas tube detectors (tables 1 and 2). The Berkeley Experiment was performed with CR39 plastics, the Kitami Experiment with nitrocellulose sheets.
- Fig. 11 Upper limits (90% CL) on the monopole flux versus monopole velocity for the multiple catalysis of proton decay in the IMB water Cherenkov detector for several values of the catalysis cross section [28-29].
- Fig. 12 Upper limits (90% CL) on the monopole flux for the single and multiple monopole catalysis of proton decays in the Mont-Blanc Experiment [22].

FIGURES CAPTIONS (Cont'd)

- Fig. 13 Signal temperature per eigenmode for a variety of materials at very low temperatures, as a function of monopole velocity. T_{eff} (today) and T_{eff} (tomorrow) indicate effective total noise temperatures that have been, or soon will be, achieved in practice. Also shown in the figure is the signal temperature for a minimum ionizing track in Cr [32].
- Fig. 14 A possible geometry for a direction-sensitive gravitational wave antenna with the capability of detecting monopoles [32].
- Fig. 15 Compilation of upper limits for classical magnetic monopole production at high energy accelerators plotted versus monopole mass. Solid and dashed lines refer to "direct" and "indirect" measurements. The new limits from the SPS $\bar{p}p$ collider ($\sigma < 3 \times 10^{-32} \text{ cm}^2$) extend up to 150 GeV.

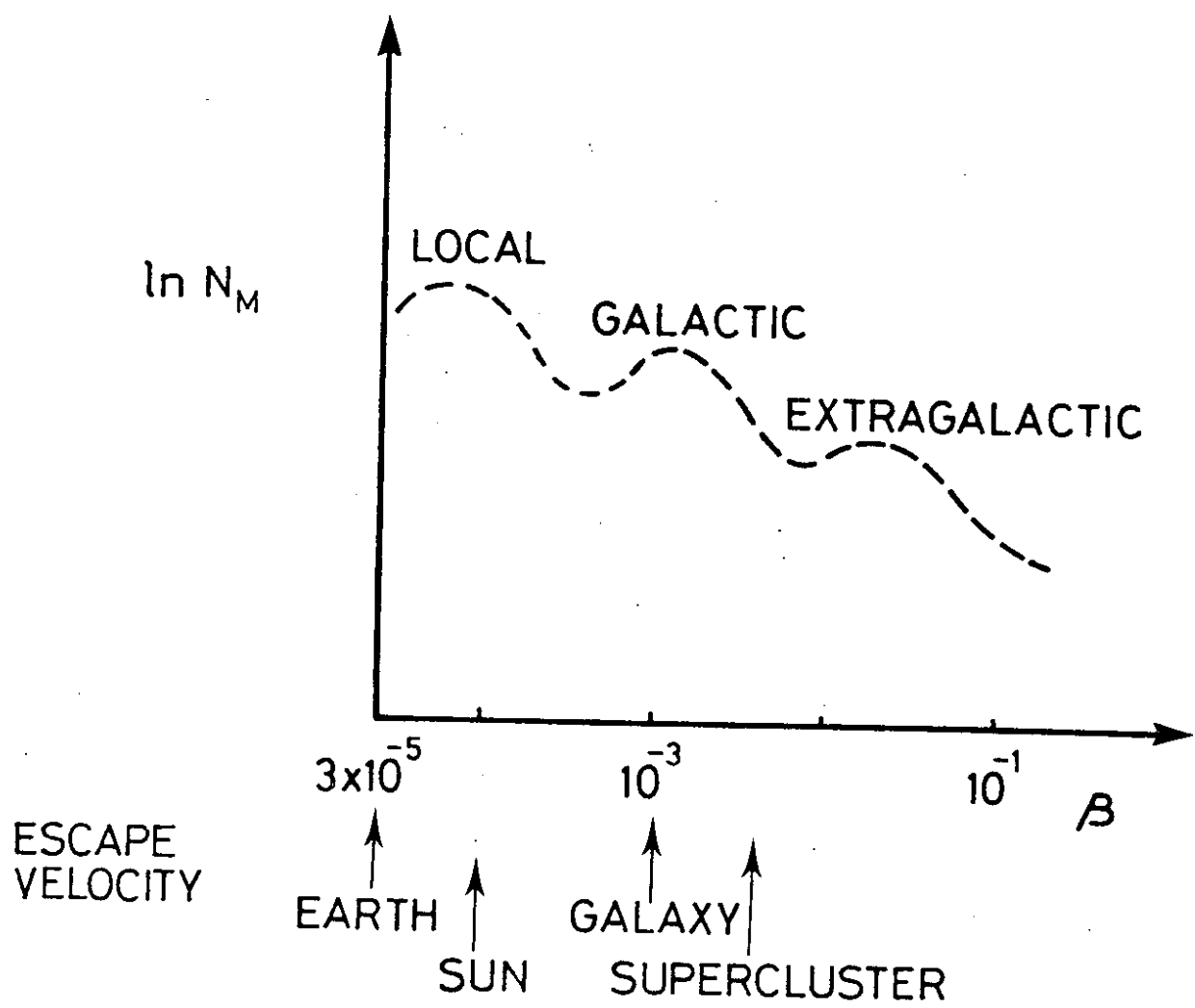


Fig. 1

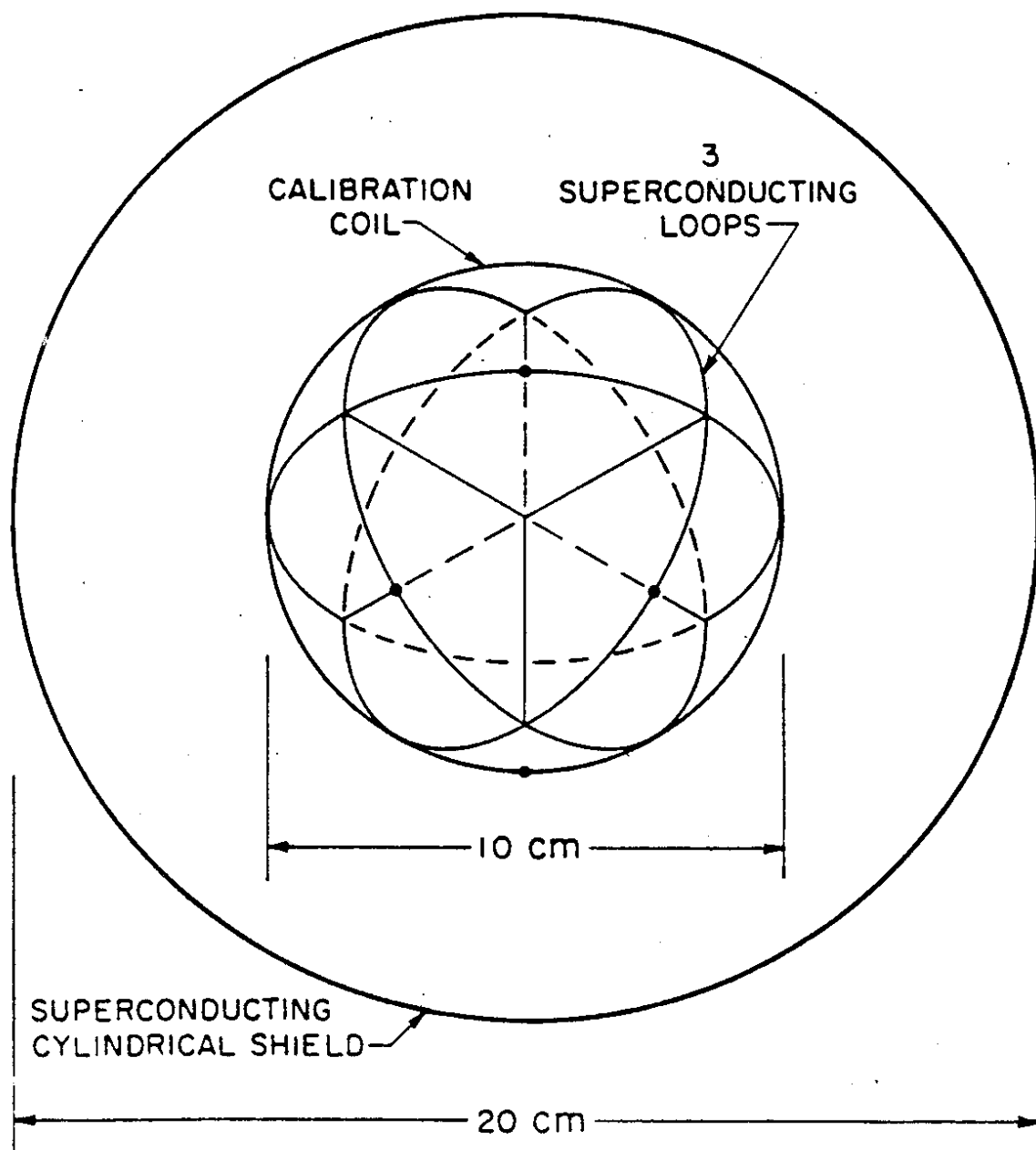


Fig. 2

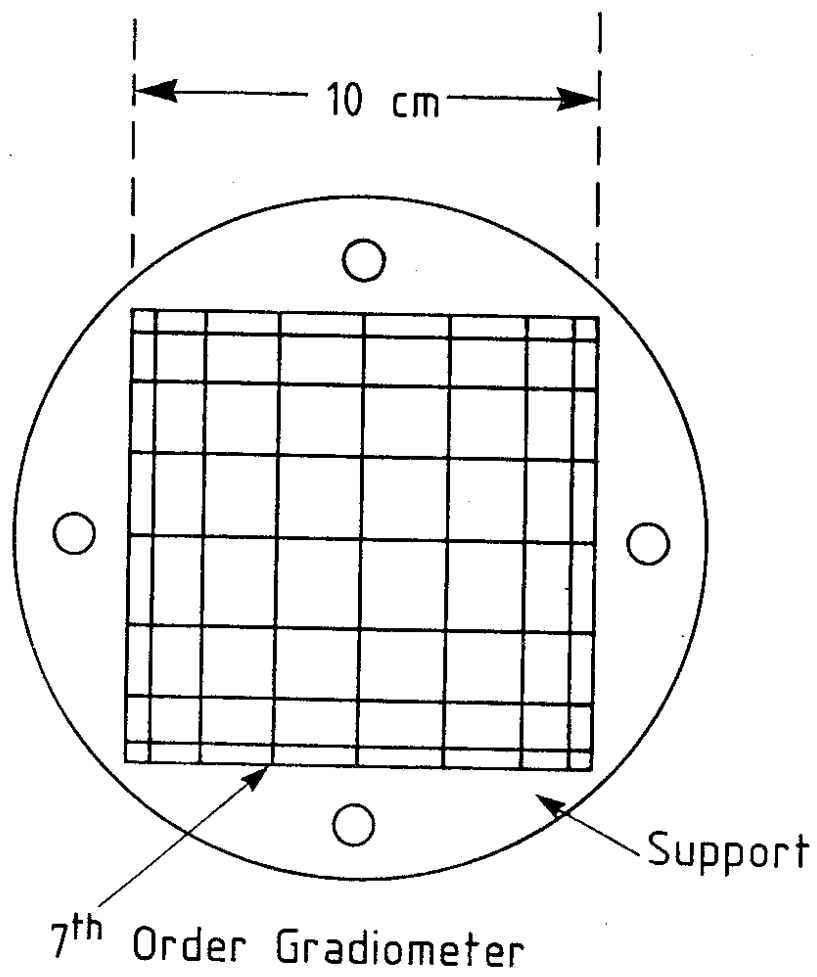


Fig. 3

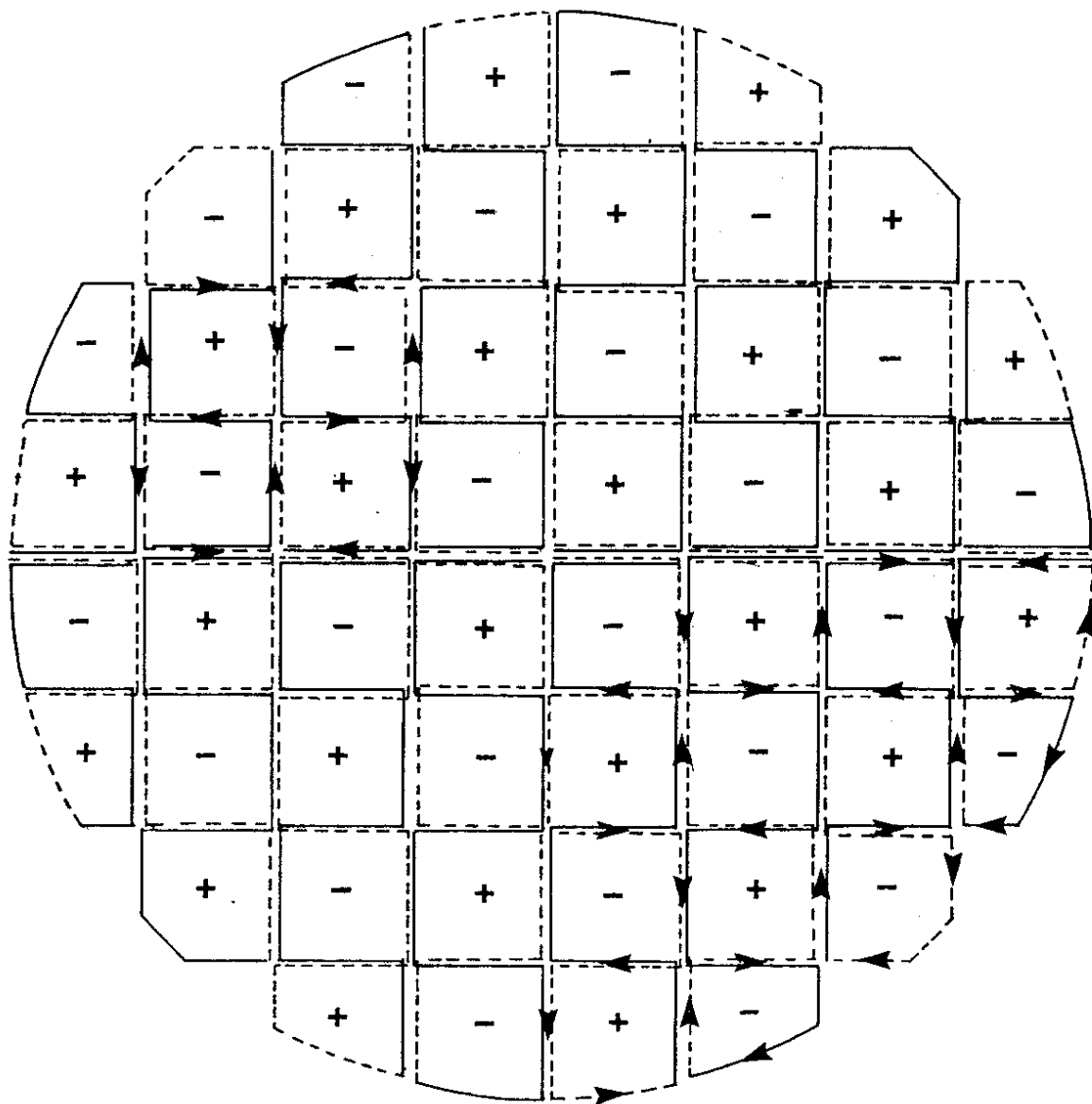


Fig. 4

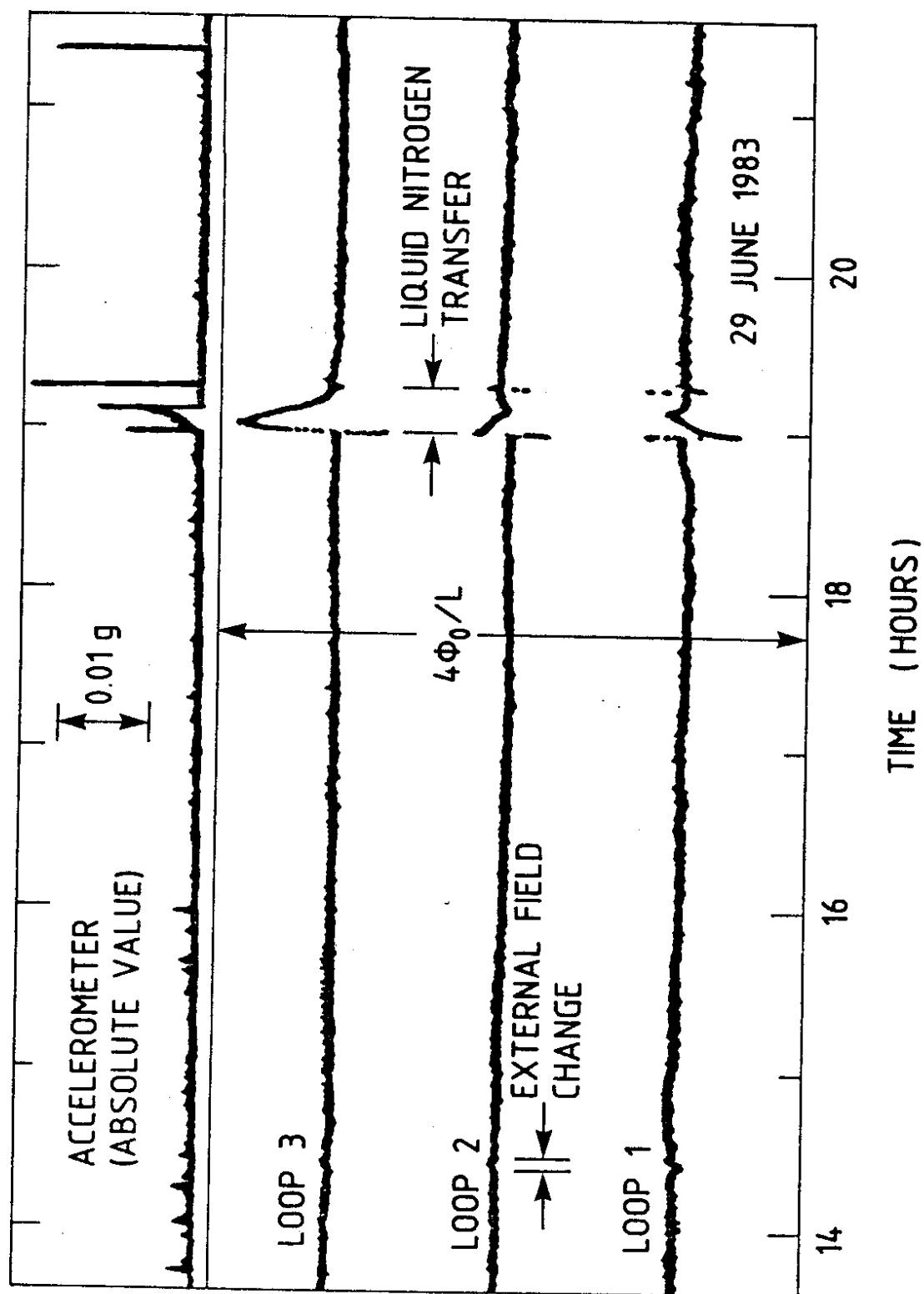


Fig. 5

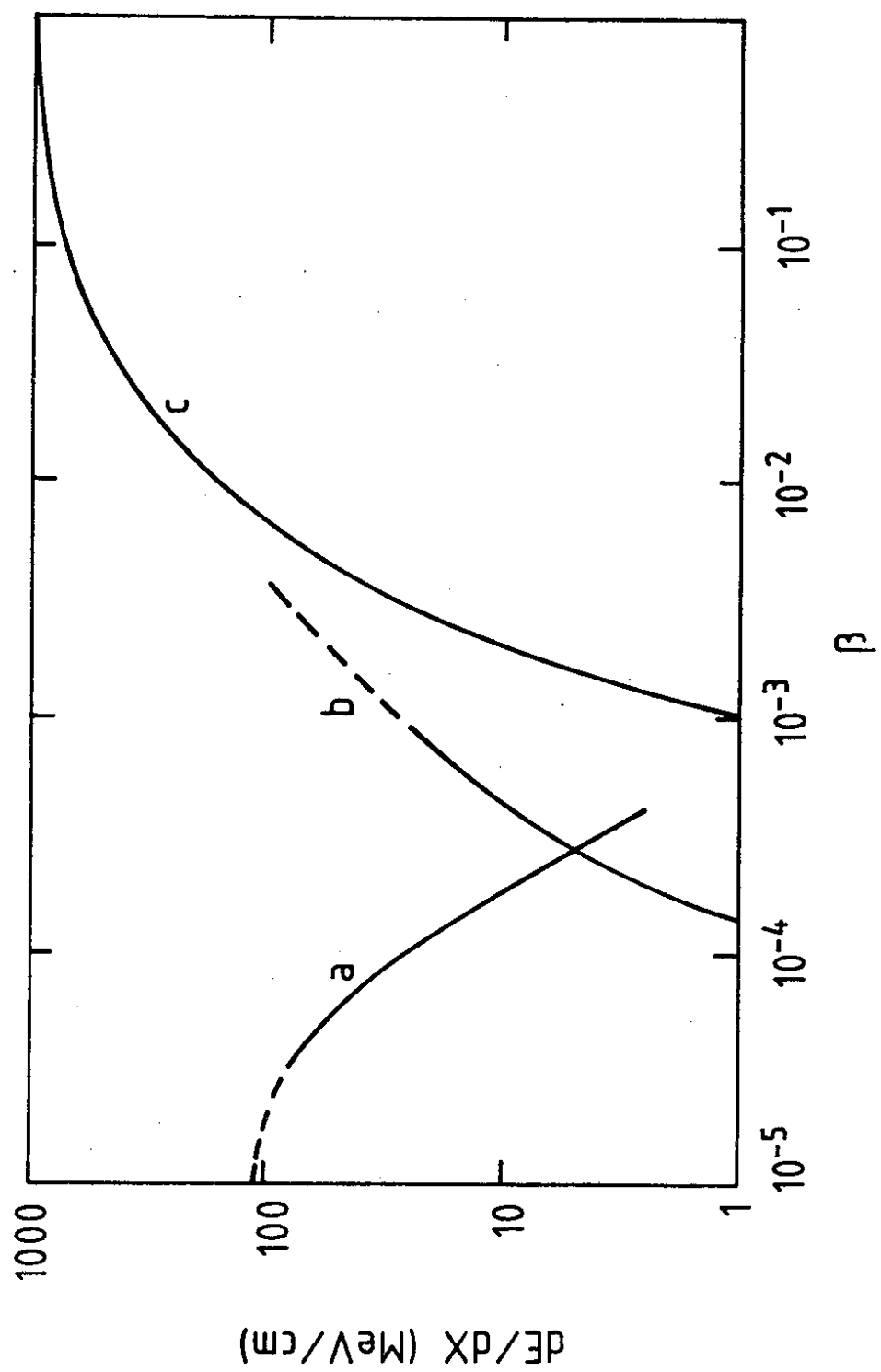


Fig. 6

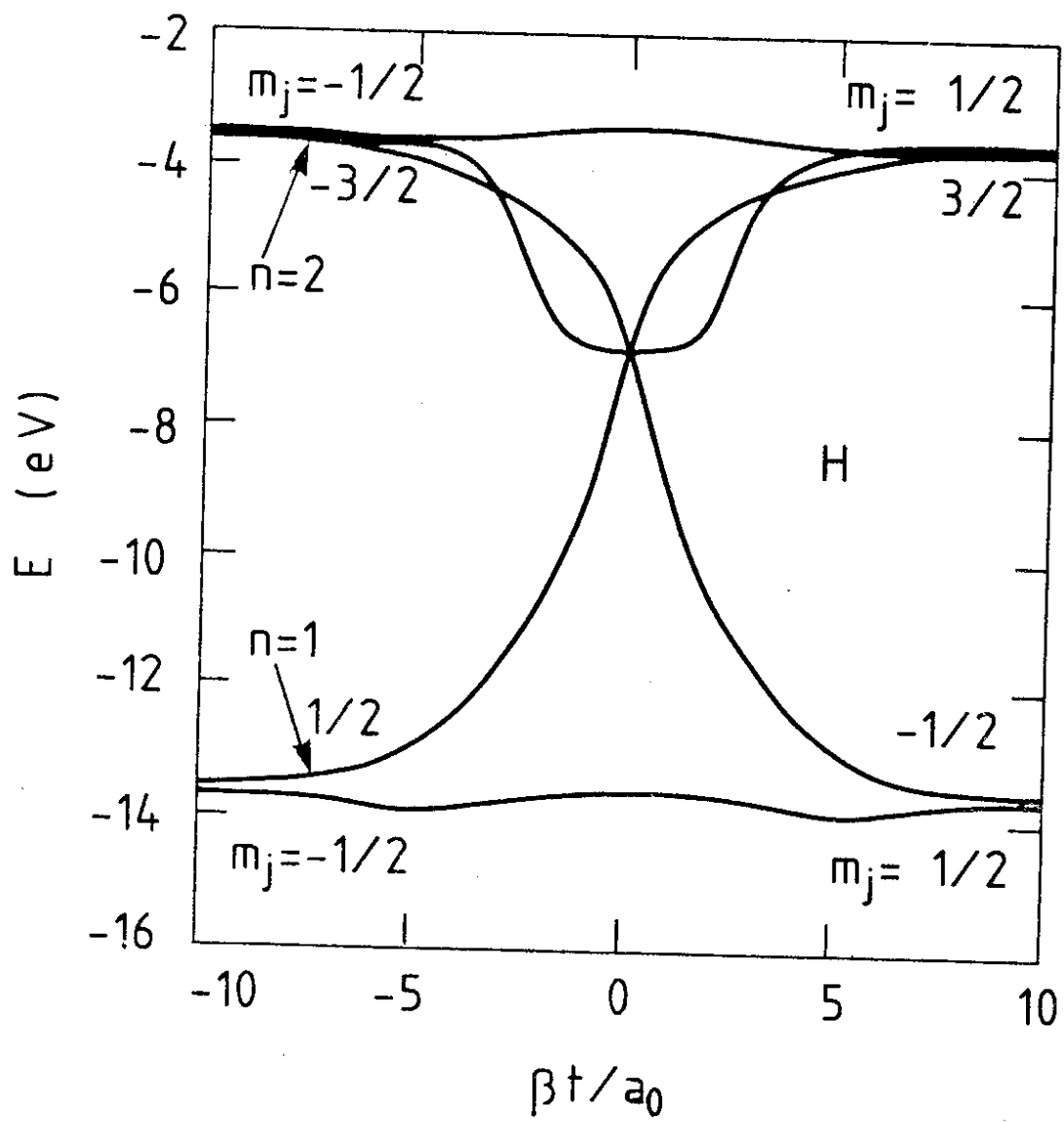


Fig. 7

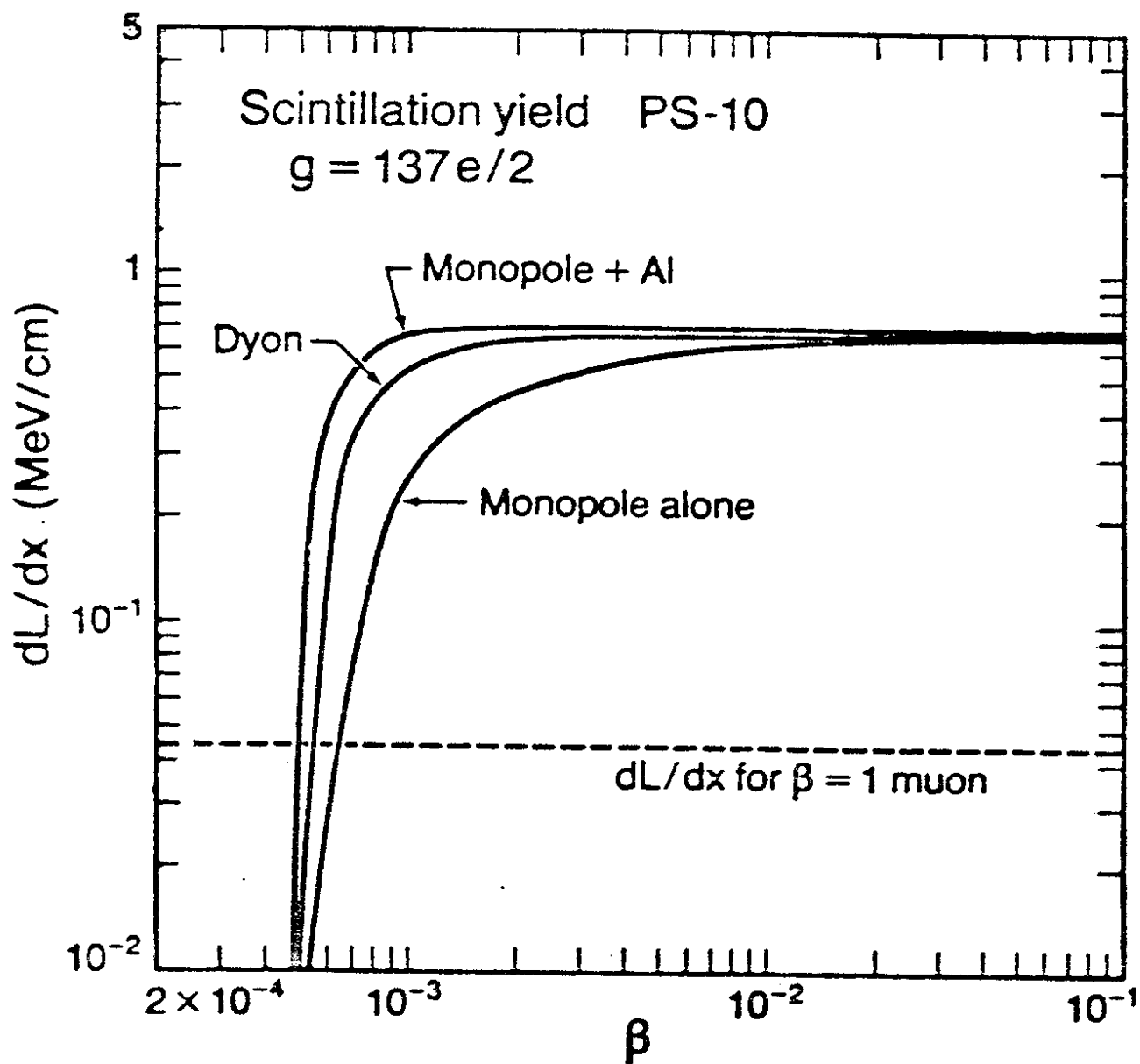


Fig. 3

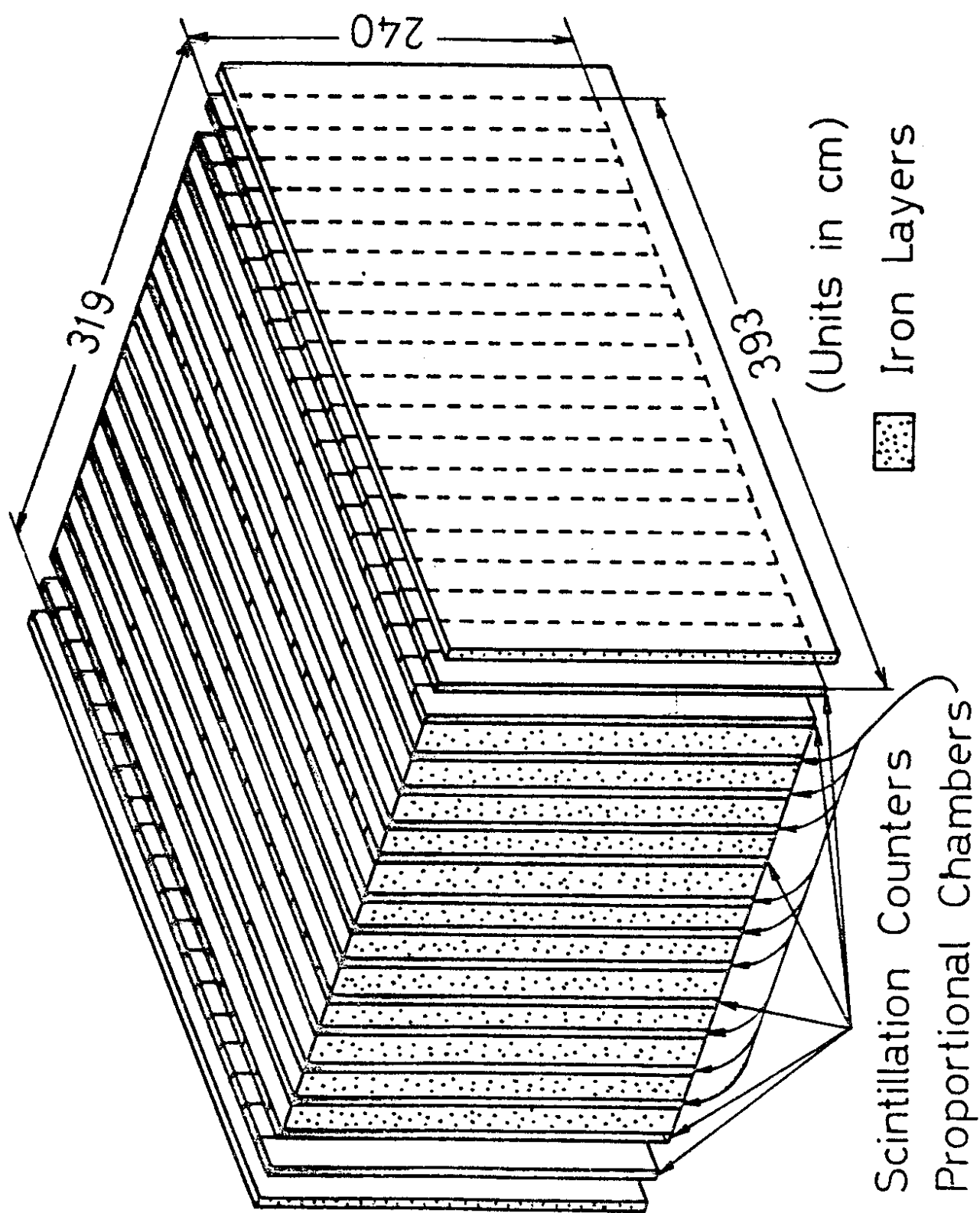


Fig. 9

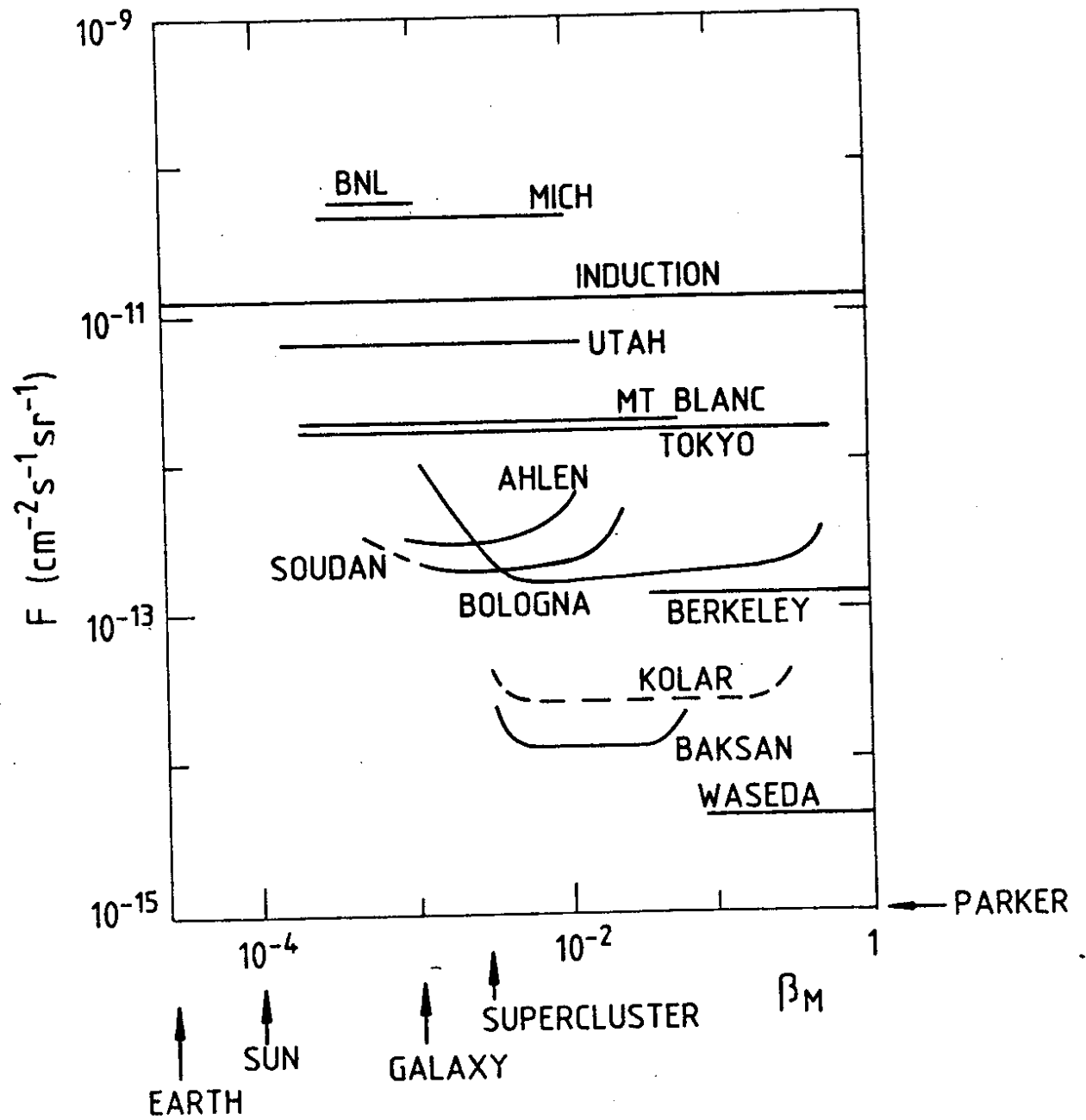


Fig. 10

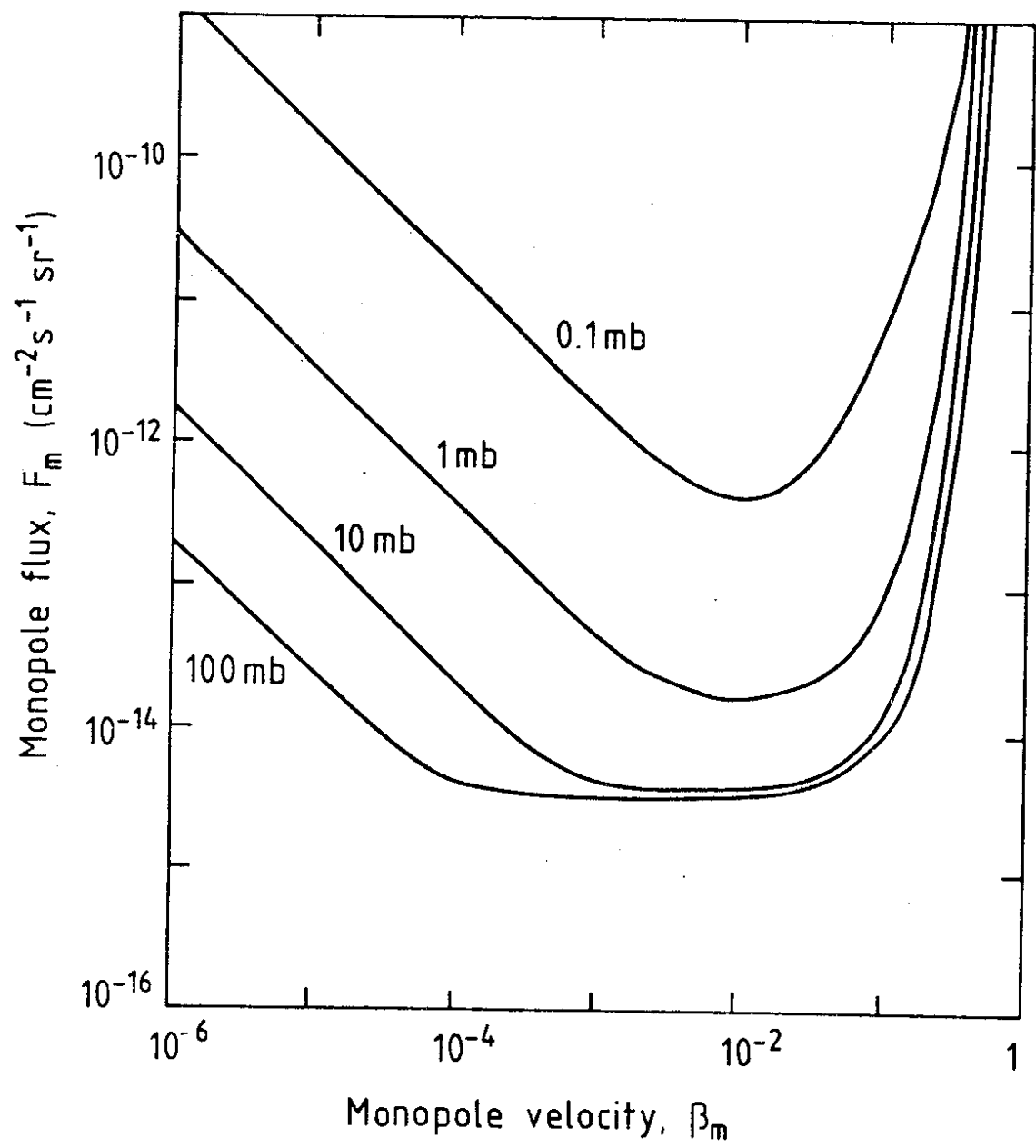


Fig. 11

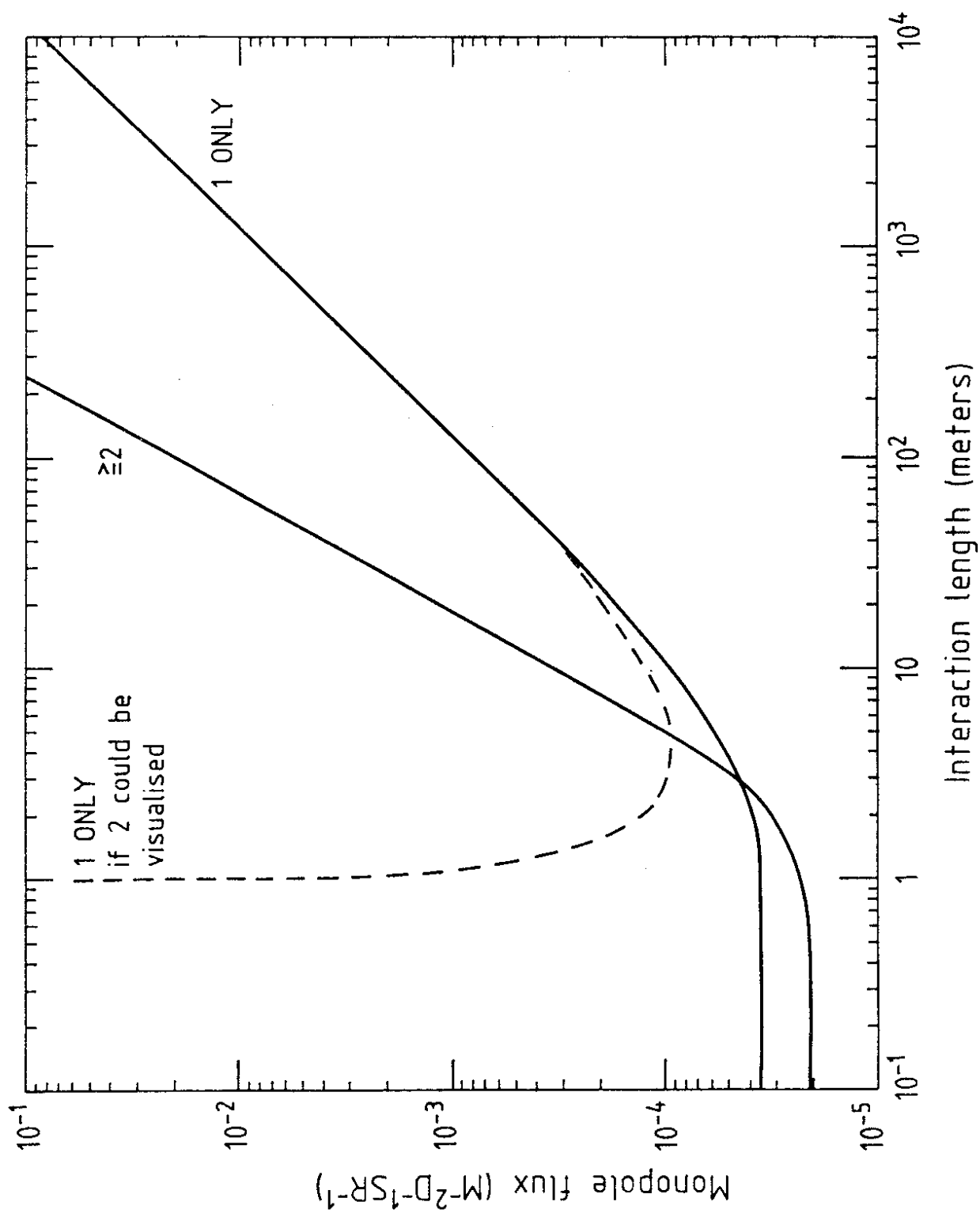


Fig. 12

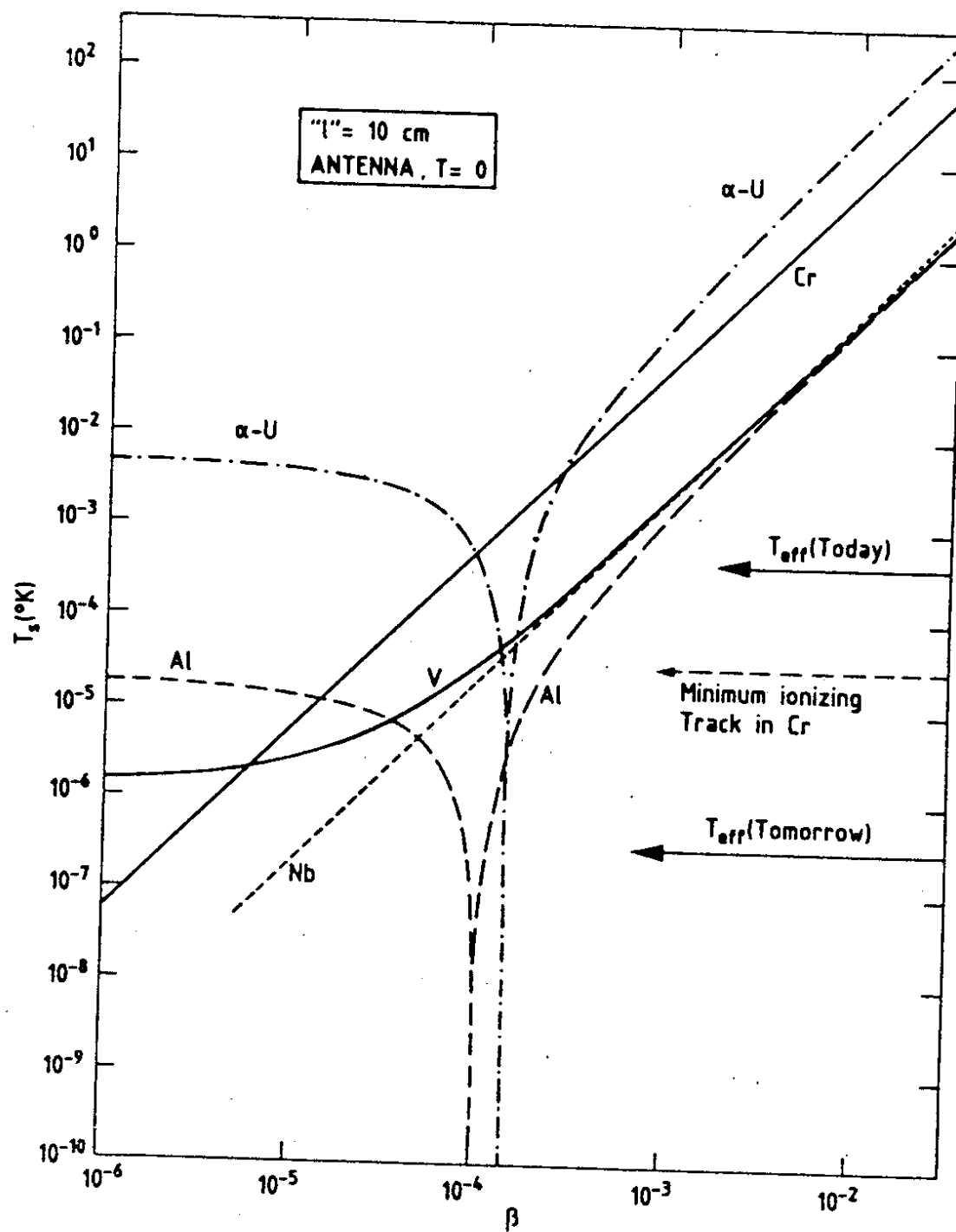


Fig. 13

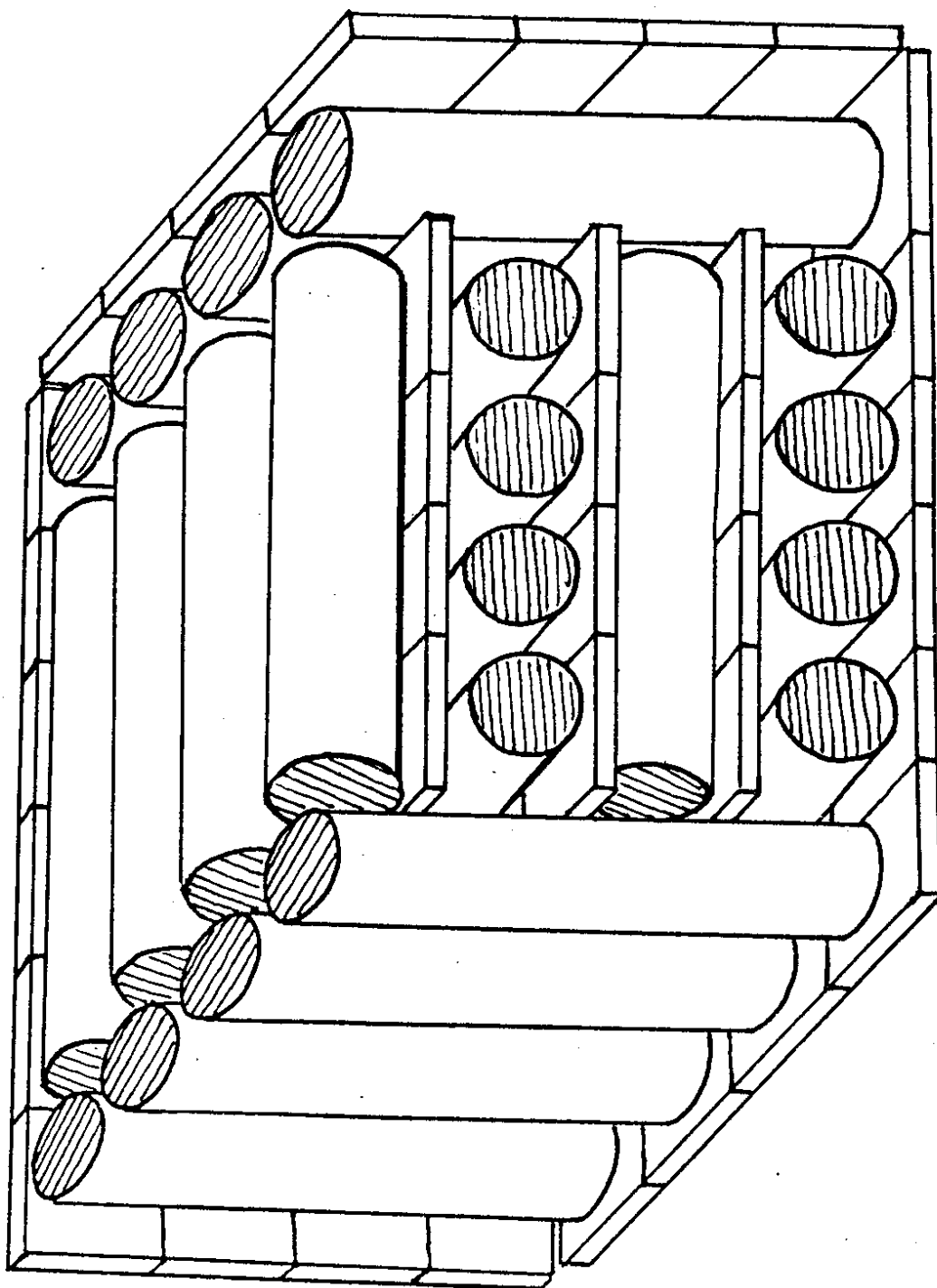


Fig. 14

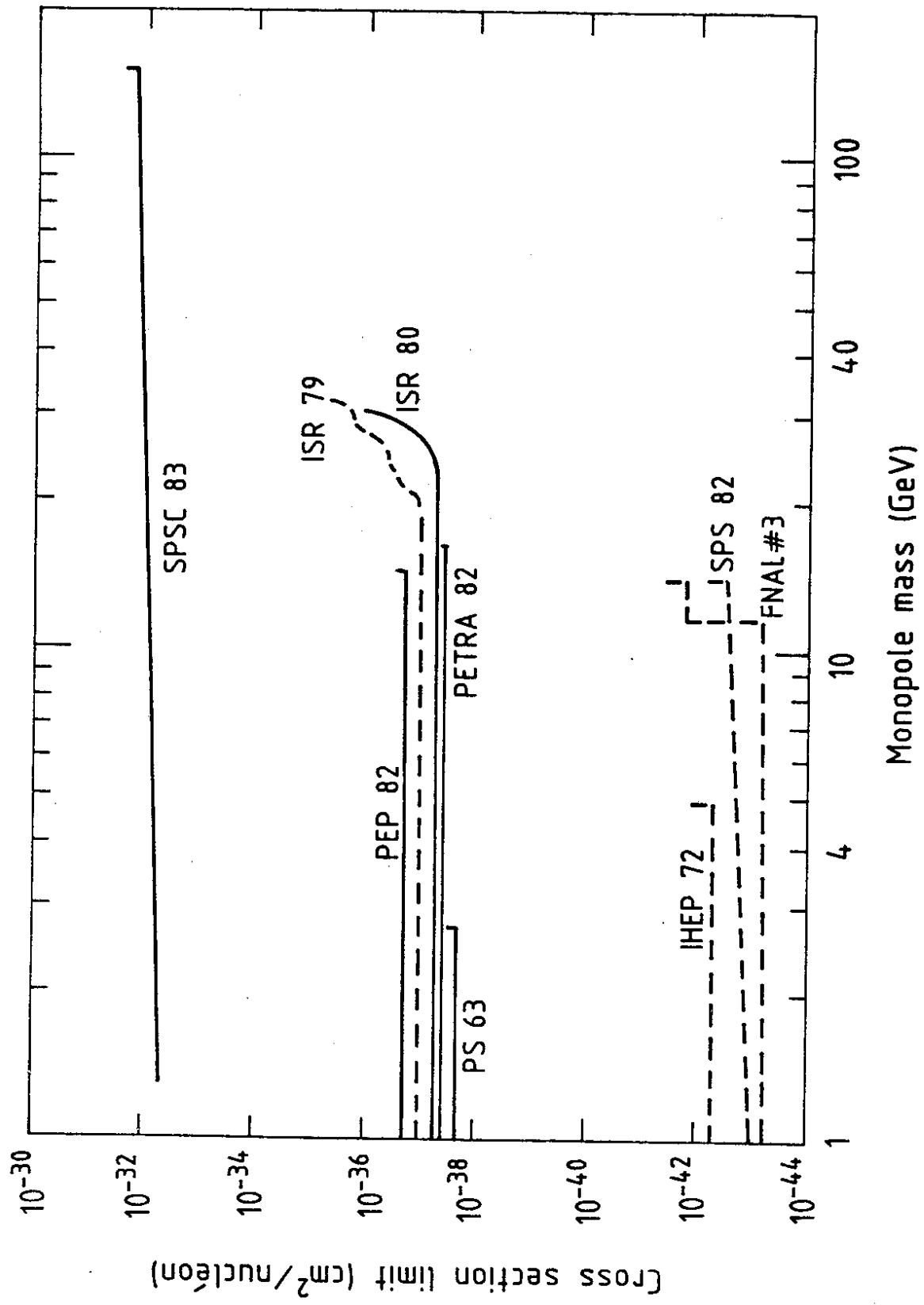


Fig. 15